

Notes

Self-Diffusion of Gelatin by Forced Rayleigh Scattering

TAIHYUN CHANG and HYUK YU*

Department of Chemistry, University of Wisconsin, Madison, Wisconsin 53706. Received April 25, 1983

We report here the results of forced Rayleigh scattering (FRS) experiments carried out with the gelatin sample that was earlier examined¹ in this laboratory by a quasi-elastic light scattering (QELS) study, for the purpose of comparing the self-diffusion coefficients obtained by FRS to the diffusion coefficients of the slow mode in QELS. A proposal has been put forth by one of us in collaboration with others¹ and by Amis and Han² that the slow mode observed in QELS of semidilute and concentrated polymer solutions may be identified with the self-diffusion process, whereas a number of others reported earlier³⁻⁷ the existence of such a mode without attributing it directly to the self-diffusion process. While there exist a firm theoretical basis⁸ and a consensus in experimental results⁹⁻¹² for identifying the fast mode of QELS as a mutual (or cooperative) diffusion process, the same cannot be said of the slow mode; a good deal of speculation about the slow-mode mechanism abounds in the literature.^{3-5,13} Furthermore, Brown et al.¹⁴ have recently called into question our identification of the slow mode by performing two separate experiments, pulsed field gradient NMR and QELS, with narrow-distribution poly(ethylene oxides), whereby they found a discrepancy of 1 order of magnitude between D_s deduced from the first experiment and the corresponding time constant inferred from the second. Our objective here is to determine D_s values of the gelatin sample by FRS over the same concentration range under experimental conditions identical with those of the earlier study¹ and compare them with the corresponding diffusion coefficients D_2 deduced from the slow-mode time constants Γ_s . In order to ensure that we have performed the FRS experiments under the same conditions, we have also carried out QELS experiments to reproduce the data by Amis et al.¹

The FRS technique was first adopted by Hervet et al.¹⁵ for a polymer self-diffusion study, which was followed by a more complete work on the same system, polystyrene in benzene, by Léger et al.¹⁶ The technique requires a certain fraction of polymer molecules being labeled by a photochromic or photobleachable moiety such that it can probe the diffusion of labeled chains dispersed in a matrix of like chains without label. As with any label technique, this too suffers from the uncertainty in sample integrity introduced by the labeling. One sure way to remove this uncertainty is to keep the labeling content to a minimum such that the final result is independent of the label concentration.¹⁶ With gelatin labeled with a photobleachable dye, fluorescein, on its lysine residues and/or the N terminus of the polypeptide chain via the thiourea linkage,¹⁷ we meet this requirement. Fluorescein is photobleachable by the 488.0-nm line of an Ar⁺ laser, and the optical grating contrast obtained by its use in aqueous medium is superior to several photochromic dyes that we have tried. Use of a photobleachable dye for the FRS experiment is not original with us but has been adopted earlier by Coutandin et al.¹⁸

Experimental Section

The pigskin gelatin sample, supplied by Rousselot S.A., Paris, was the same one used by Amis et al.¹ Appropriately weighed samples of gelatin to make final weight percents of 0.2, 1, 2, 5, 10, and 20 were dissolved in deionized water at 35 °C to make 10 g of each solution, and an aliquot (10 μ L) of 32 mM acetone solution of fluorescein isothiocyanate (Sigma) was added to each solution, which was then allowed to stand at the same temperature with occasional stirring for at least 2 h. The labeling yield appeared to be quantitative as judged by the absence of any free dye band in an electrophoresis band pattern on polyacrylamide-SDS gels. The bound-label position, either on an interior lysine residue or on the N terminus of the chain, is not characterized. Since the lysine content in gelatin is in the range of 25-27 per 1000 residues, depending on the gelatin sources,^{19,20} it is likely that 1 of 8-9 lysine residues in a chain ($M_n = 35\,000$; DP ≈ 350) is labeled by fluorescein. The average labeling yield in the largest case, with 0.2% solution, amounts to about 6 dye molecules per every 10 polymer chains and it is reduced by 100-fold in the smallest case, with 20% solution. QELS measurements were made with two samples of 0.2% solution, one with the indicated average labeling yield and the other without any labeling, and the results were found to be indistinguishable, indicating no detectable effect by the label on the average Stokes radius.

The FRS apparatus used here has been described elsewhere.²¹ The sample cell holder is constructed of a copper block through which heat-exchange liquid circulates from a constant-temperature bath (Lauda) to control the temperature of the cell to within 0.2 °C. Though the data acquisition scheme is the same as before, the analysis method is slightly different. The photomultiplier tube output $V(t)$ due to the time-varying diffraction intensity of the reading beam is analyzed by a model function

$$V(t) = (Ae^{-t/\tau} + B)^2 + C^2 \quad (1)$$

where the four parameters determined by a nonlinear least-squares fitting routine on a Harris/7 computer are A , the preexponential amplitude of the diffracted optical field, B , the coherent scattering background of the optical field, τ , the relaxation time of the diffracted optical field, and C^2 , the background intensity due to incoherent scattering and stray light.

The instrument used for QELS is the same one as in the report by Amis et al.¹ The concentration range covered for QELS extends further into dilute solution than in their study in order to establish the translational diffusion coefficient at infinite dilution D_0 . The fast and slow modes were analyzed separately by the second-order cumulant method.²² Since a changeover from homodyne to heterodyne beating for the fast mode should take place¹ as concentration is increased but we cannot be sure at what concentration without performing a separate heterodyne experiment, we assume that both modes are detected by the homodyne beating mechanism. This is to be contrasted with the way QELS data were earlier¹ interpreted by assuming heterodyne detection for the fast mode and homodyne detection for the slow mode.

Results and Discussion

In Figure 1, we display the observed linear dependence of the relaxation time τ on the squared fringe spacing d^2 , as expected for any translational diffusion process of photolabels, according to

$$\tau = d^2 / 4\pi^2 D_s \quad (2)$$

The slope of the straight line increases progressively with gelatin weight percent as indicated. The values of D_s calculated by eq 2 are collected in Table I, where the uncertainties represent 95% confidence limits deduced from the slopes of the plots in Figure 1. In the inset, we show a typical rise-decay profile of the diffraction signal

Table I
Various Diffusion Coefficients Obtained by FRS and QELS at Different Concentrations of Gelatin at 35 °C

$W_2, \%$	D or $D_c \times 10^7, ^a$ cm^2/s	$D_c \times 10^7, ^b$ cm^2/s	$D_s \times 10^8, ^c$ cm^2/s	$D_2 \times 10^8, ^d$ cm^2/s	$A(\text{fast})/A(\text{slow})^e$
0.1	1.9 ± 0.5				
0.2	2.0 ± 0.3		21 ± 6		
1	1.8 ± 0.2		19 ± 2	3.6 ± 0.5	0.62/0.38
2	1.7 ± 0.2	3.28	15 ± 2	3.1 ± 0.4	0.51/0.49
5	1.7 ± 0.2	3.88	10 ± 1	1.7 ± 0.2	0.36/0.64
10	2.1 ± 0.4	5.06	4.7 ± 0.3	0.63 ± 0.09	0.20/0.80
20	3.7 ± 0.5	6.38	0.87 ± 0.05	0.08 ± 0.01	0.07/0.93

^a All deduced from Γ_f of QELS assuming a homodyne detection mechanism. ^b Those of Amis et al. from their Γ_f assuming a heterodyne detection mechanism. ^c Obtained from FRS measurements. ^d Deduced from Γ_s of QELS assuming a homodyne detection mechanism. ^e Ratio of autocorrelation amplitudes of the fast and slow modes at 90° scattering angle.

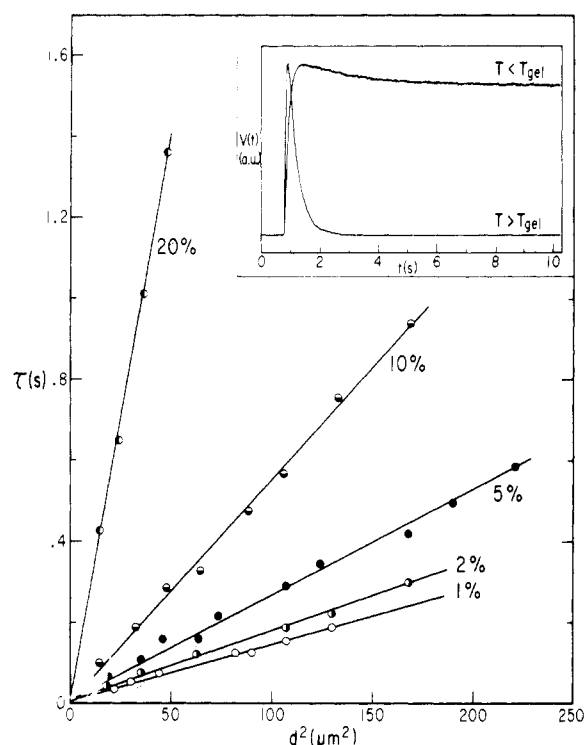


Figure 1. Decay relaxation time τ of the diffracted optical field plotted against squared fringe spacing d^2 in FRS experiments, where gelatin weight percent is indicated for each sample. A data set for the 0.2% sample is not shown because it is similar to that of the 1% sample although the scatter is greater as shown by the error bar on the D_s value in Figure 2. In the inset, a rise-decay profile of the diffraction signal with the 10% sample at 35 °C is contrasted to a profile obtained at 22 °C with the same sample. The observed persistence of the diffraction signal at 22 °C indicates that the self-diffusion process is arrested in the gel by restraining the polymer chains into a network.

at 35 °C, which is above the gel temperature of this gelatin sample. On the same graph, we show how the diffraction signal at 22 °C, a temperature below the gel point, remains practically unchanged. Since the sample has gelled at this temperature, there should be no chain self-diffusion. Thus, the imposed optical grating cannot be erased by the mass diffusion mechanism of photobleached labels; hence the diffraction signal is no longer transient as long as fluorescein photobleaching is irreversible. A small initial decay in the diffraction signal is tentatively attributed to gel network dynamics, which may be reduced by lowering temperature. The difference in the rise parts of the two is ascribed to the photobleaching rate difference over a temperature interval of 13 °C. Notwithstanding these minor details, the two diffraction signal profiles make it certain that the self-diffusion process can be arrested by restraining the polymer chains into a network. This cor-

responds to the earlier observation by Amis et al. that the slow mode of QELS disappears completely in a gel at 20 °C whereas the fast mode due to the cooperative diffusion remains unaffected.

As stated before, we deduce the diffusion coefficient D , which becomes the cooperative diffusion coefficient D_c at $c > c^*$, from the fast mode of QELS. Assuming a homodyne detection mechanism such that the decay rate of the autocorrelation function $G^{(2)}(\tau)$ is $2\Gamma_f$, we can deduce the diffusion coefficient D or D_c from the definition $\Gamma_f = D\kappa^2$, κ being the scattering wave vector. These are also listed in Table I. We have noted that Γ_f depended on the choice of sample time $\Delta\tau$ in acquiring $G^{(2)}(\tau)$, most likely due to the broad molecular weight distribution of the gelatin, and it did not converge to a well-defined value independent of $\Delta\tau$. We therefore chose to determine Γ_f with a single sample time $\Delta\tau$ for all concentrations at a given scattering angle, namely, 1 μs per channel at 90° scattering angle on a 64-channel correlator, which amounts to about 2 relaxation times for the entire time range for a particular sample, and $\Delta\tau$ variation with the scattering angle was effected under the condition of $\kappa^2\Delta\tau = \text{constant}$. Hence Γ_f values are subject to considerable ambiguity and the resulting D or D_c values are less than firmly established; we might have perhaps as much as a factor of 2 in variation of mean diffusion coefficient, depending on $\Delta\tau$. The listed values of D or D_c in Table I differ from those in Amis et al. by about a factor of 2, mainly due to the different assumptions for the QELS detection mechanism but also partly because of the choice of $\Delta\tau$. A ready comparison of the difference is afforded by listing their D_c values in Table I. As for the determinations of D_2 from Γ_s , we have fully reproduced theirs, and our D_2 values are listed in the fifth column of Table I. In the last column of the table we also list the ratios of amplitudes of the autocorrelation function $G^{(2)}(\tau)$ of the fast and slow modes; by amplitude, we mean the preexponential term of each decay mode.

In Figure 2, we show a plot of D_s vs. W_2 , gelatin weight percent, together with D_2 and D_c (or D) plotted against the same W_2 . The D_s value is larger than D_2 by about a factor of 5 at $W_2 = 1\%$ and it increases progressively to about 10 at $W_2 = 20\%$. The arrow at the top indicates the approximate overlap concentration c^* , taken equal to the reciprocal intrinsic viscosity of the gelatin sample, $[\eta] = 22 \text{ mL/g}$. Thus, only those data points to the right of the arrow should be regarded as D_c because they alone are in the semidilute regime whereas those to the left of the arrow are the translational diffusion coefficients D in the dilute solution regime, which appear to converge smoothly with D_s to reach the infinite dilution limit; i.e., $\lim_{c \rightarrow 0} D = \lim_{c \rightarrow 0} D_s = D_0$.

To the extent that we took care to minimize likely artifacts of FRS experiments, we hope that these determinations of the self-diffusion coefficients are unambiguous.

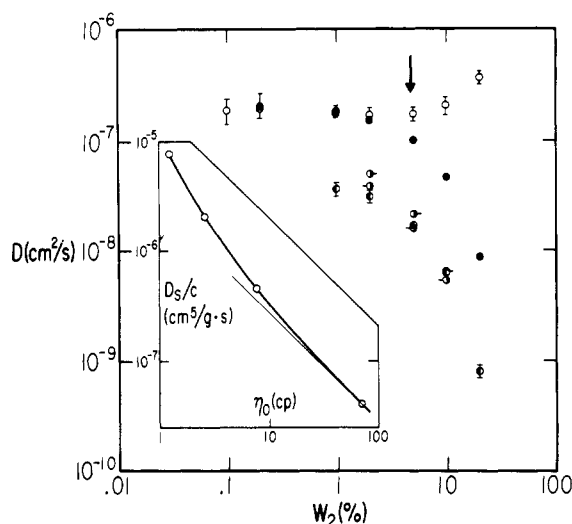


Figure 2. Double-logarithmic plot of different diffusion coefficients against weight % of gelatin, W_2 . Self-diffusion coefficients D_s obtained from the slopes of the straight lines in Figure 1 are shown by filled circles, D or D_c obtained from the fast mode of QELS by open circles, and D_2 from the slow mode of QELS by left-half-filled circles. Error bars are shown when 95% confidence intervals exceed the size of the data points. When our D_2 values differ from the corresponding ones by Amis et al., the latter are shown by right-half-filled circles with pips whose directions distinguish the two different data analysis schemes, single-exponential and second-order cumulant fits. The arrow at the top indicates the concentration equaling the reciprocal of the intrinsic viscosity, which may be taken as the overlap concentration, $c^* \approx 1/[\eta] = 0.045$ g/mL. In the inset, D_s/c is plotted against steady shear viscosity (Amis et al.) on a double-logarithmic scale, where the curve is drawn smoothly over the data points simply to indicate the trend and the line is drawn with a slope of -1 , representing the Rouse chain behavior.

If so, the slow mode of QELS is not the self-diffusion process though it seems to represent some measure of the process as manifested by its approximately parallel concentration dependence and its disappearance in gel. The concentration and molecular weight dependences of D_2 for polystyrenes in both good² and θ solvents²³ were also found to mimic those expected for D_s . Precisely what measure of the self-diffusion process the slow mode represents we cannot say. In any event, we have to agree with Brown et al.¹⁴ in disputing the identification of the QELS slow mode with the self-diffusion process, but without proposing an alternative responsible for the mode. There is now an agreement among us²⁴ that our earlier identification of the slow mode needs to be reconsidered.

We close this report by noting that the D_s values at $c > c^*$ appear to approach the behavior of Rouse chains relative to concentration c and steady shear viscosity η_0 ;

namely, $D_s/c \propto 1/\eta_0$. This is shown in the inset of Figure 2, where D_s/c is plotted against η_0 on a double-logarithmic scale using η_0 values given by Amis et al. A thin line tangent to the lowest data point (20%) has the slope of -1 . If we connect the data points at 5% and 20%, then the slope is -1.2 . This is to be contrasted with the finding of D_2 being proportional to $1/\eta_0$ reported in the earlier paper.

Acknowledgment. This work was supported in part by grants from the Eastman Kodak Co. and the National Science Foundation (Polymers Program, DMR 7908652). We gratefully acknowledge fruitful discussions with Dr. Eric J. Amis and Prof. John D. Ferry, who also graciously provided the gelatin sample. We also thank our colleagues J. A. Wesson, M. R. Landry, and J. M. Yohanan for their help.

References and Notes

- (1) Amis, E. J.; Janmey, P. A.; Ferry, J. D.; Yu, H. *Macromolecules* **1983**, *16*, 441. *Polym. Bull.* **1981**, *6*, 13.
- (2) Amis, E. J.; Han, C. C. *Polymer* **1982**, *23*, 1403.
- (3) Chu, B.; Nose, T. *Macromolecules* **1980**, *13*, 122.
- (4) Nishio, I.; Wada, A. *Polym. J.* **1980**, *12*, 145.
- (5) Mathiez, P.; Mouttet, C.; Weisbuch, G. *J. Phys. (Paris)* **1980**, *41*, 519.
- (6) Yu, T. L.; Reihanian, H.; Jamieson, A. M. *Macromolecules* **1980**, *13*, 1590.
- (7) Southwick, J. G.; Jamieson, A. M.; Blackwell, J. *Macromolecules* **1981**, *14*, 1728.
- (8) de Gennes, P.-G. *Macromolecules* **1976**, *9*, 587.
- (9) Adam, M.; Delsanti, M. *Macromolecules* **1977**, *10*, 1229.
- (10) Munch, J. P.; Candau, S.; Herz, J.; Hild, G. *J. Phys. (Paris)* **1977**, *38*, 971.
- (11) Munch, J. P.; Lemaréchal, P.; Candau, S.; Herz, J. *J. Phys. (Paris)* **1977**, *38*, 1499.
- (12) Jarry, J.-P.; Patterson, G. D. *Macromolecules* **1981**, *14*, 1281.
- (13) Chu, B. In "Scattering Techniques Applied to Supramolecular and Nonequilibrium Systems"; Chen, S.-H., Nossal, R., Eds.; Plenum Press: New York, 1980; p 231.
- (14) Brown, W.; Johnsen, R. M.; Stilbs, P. *Polym. Bull.* **1983**, *9*, 305.
- (15) Hervet, H.; Léger, L.; Rondelez, F. *Phys. Rev. Lett.* **1979**, *42*, 1681.
- (16) Léger, L.; Hervet, H.; Rondelez, F. *Macromolecules* **1981**, *14*, 1732.
- (17) Nairn, R. C. "Fluorescent Protein Tracing", 2nd ed.; Williams and Wilkins: Baltimore, 1964.
- (18) Coutandin, J.; Sillescu, H.; Voelkel, R. *Makromol. Chem., Rapid Commun.* **1982**, *3*, 649.
- (19) Rose, P. I. In "The Theory of the Photographic Process", 4th ed.; James, T. H., Ed.; Macmillan: New York, 1977; Chapter 2.
- (20) Veis, A. "Macromolecular Chemistry of Gelatin"; Academic Press: New York, 1964; p 6.
- (21) Wesson, J. A.; Takezoe, H.; Yu, H.; Chen, S. P. *J. Appl. Phys.* **1982**, *53*, 6513.
- (22) Koppel, D. E. *J. Chem. Phys.* **1972**, *57*, 4814.
- (23) Amis, E. J.; Han, C. C.; Matsushita, Y. *Polymer*, in press.
- (24) Ferry, J. D.; Amis, E. J.; Janmey, P. A., private communication.